Spectropolarimetry of a Sunspot at 1565nm: Penumbral Moving Magnetic Features

M.J. Penn[1], S.A. Jaeggli[2], C.J. Henney[1], S.R. Walton[3] and S.H. Luszcz[4]
[1] *National Solar Observatory * , 950 N Cherry Av, Tucson AZ 85719*

[2] *University of Arizona, Department of Astronomy, 933 N Cherry Av, Tucson AZ 85721-0065*

[3] *California State University Northridge, Department of Physics and Astronomy, 18111 Nordhoff St, Northridge CA 91330-8268*

[4] *Cornell University Department of Physics, 109 Clark Hall, Ithaca, NY 14853-2501*

Abstract. Full Stokes I, Q, U and V measurements of the active region NOAA 10008 were taken on 24 June 2002 at the National Solar Observatory (NSO) Kitt Peak McMath/Pierce (McM/P) solar telescope using the California State University Northridge (CSUN)/ NSO HgCdTe IR camera and polarimeter at 1565nm. Instrumental polarization effects are apparent in Stokes spectra. These polarization cross-talk terms are computed and removed using an indirect correction method, and this method compares favorably with predictions from a telescope polarization model. The Fe I g=3 1564.8nm Stokes profiles are then inverted with a Skumanich and Lites technique to measure photospheric magnetic field parameters. A sequence of scans covering several hours of time shows evolution of the magnetic field. Many moving magnetic features are observed for the first time inside the sunspot penumbra. Some of these features can be traced to cross the penumbral boundary and move across the sunspot moat, and all of these features have velocities and azimuth angles similar to other moving magnetic features observed in the moat.

1. Introduction

Observations of the full Stokes profiles of solar absorption lines in the visible are now routinely used to measure the vector magnetic fields on the Sun (Elmore *et al.* 1992, Mickey *et al.* 1996, and Sankarasubramanian *et al.* 2004) and some investigators have used near-IR Fe I lines at 1565 nm to investigate the line-of-sight and the vector magnetic fields on the Sun (Kopp & Rabin, 1992, Lin, 1995, Bellot Rubio *et al.* 2000, Schlichemaier & Collados, 2002, and Mathew *et al.* 2003). With telescopes that have oblique reflections before the polarization

* Operated by the Association of Universities for Research in Astronomy, Inc. (AURA), under cooperative agreement with the National Science Foundation

analysis is made, cross-talk between the Stokes states can make the observed Stokes profiles very different from the true Stokes profiles. Correcting this instrumental polarization is necessary before the Stokes profiles can be analyzed. Polarization models, direct, or indirect empirical techniques have been used by a number of authors to recover the true Stokes profiles from observed profiles (Makita and Nishi 1970, Balasubramaniam, Venkatakrishnan and Bhattacharyya 1985, Capitani *et al.* 1989, Elmore *et al.* 1992, Kuhn *et al.* 1994, and Collados 2003).

After obtaining the instrument corrected Stokes profiles, a number of techniques are used for determining the solar vector magnetic field from photospheric lines. The range of complexity runs from determination of an average magnetic field in the solar atmosphere with simple profile integration (Walton & Chapman, 1996) or with line fitting using a source function linear with optical depth (Skumanich & Lites, 1987a), to line-profile inversion methods used to measure solar parameters at many levels in the atmosphere (Ruiz Cobo & del Toro Iniesta, 1992).

The magnetic fields observed in the sunspot penumbra show changes with azimuthal angle around the sunspot. Title *et al.* (1993) used line-of-sight magnetograms to show magnetic inclination angle variations around the sunspot, while Lites *et al.* (1993) showed that the more vertical fields have larger inherent field strengths using an analysis of vector field measurements. These uncombed penumbral magnetic fields remained stable during 30 minutes of observation in the Lites *et al.* (1993) data, although there seemed to be a relationship between inclination variations at the edge of the penumbra and the moving magnetic features (MMF) seen in the photosphere outside of the sunspot (Harvey & Harvey, 1973). Lites *et al.* (1998) studied temporal fluctuations below 2.39 mHz in penumbral continuum intensity, magnetic field strength, and field inclination. These maps reveal distinct features travelling radially inward at a few tenths of a km s^{-1} in the inner penumbra and umbra, and radially outward in the outer penumbra and surrounding quiet sun. Zhang, Solanki & Wang (2003) observed that 7 of 144 MMFs first appeared within the sunspot penumbral boundary. Inward and outward penumbral migrations were also observed by Bovelet and Weihr (2003) in images of G-band bright points. They found an inward, 0.8 km s^{-1} flow of penumbral bright structures in the inner penumbra, as well as a less organized outward flow of the same magnitude of penumbral bright and dark structures in the outer penumbra.

In this work a time sequence of Stokes measurements of the Fe I 1564.8nm spectral line in the main sunspot of NOAA 10008 on 24 June 2002 (section 2) are corrected for instrumental effects (section 3) and then fit with a linear source function model (section 4) to derive a

time sequence of magnetic field measurements. Temporal variations of the magnetic inclination are seen in the penumbra and compared with MMFs seen outside of the sunspot. Many penumbral moving magnetic features (pMMFs) are seen (in both magnetic inclination angle and magnetogram time sequences) which travel through the outer half of the penumbra and then continue across the sunspot moat as a standard MMF.

2. Observations

The National Solar Observatory (NSO) 1.5m McMath-Pierce telescope on Kitt Peak is described in detail by Pierce (1964) and infrared observations have been made with the main spectrograph by a number of authors. In the observations discussed here, the main heliostat fed the main spectrograph, which used the infrared grating, and telescope scanning was done by changing the main heliostat pointing. The joint California State University Northridge (CSUN) - NSO infrared camera is a HgCdTe based system, using a 256x256 pixel detector and was described in Penn *et al.* (2003).

In these observations the spectral dispersion was 0.0056 nm per pixel and the spectral field-of-view covered about 1.4 nm. The spatial dispersion was 0.30 arcsec per pixel along the spectrograph slit, and the scan resulted in 0.99 arcsec steps perpendicular to the slit. The slit was oriented along the geocentric north-south direction, scanning progressed from geocentric east to west, and the scans covered 76 (N/S) by 197 (E/W) arcseconds on the solar surface. The scans were centered on active region NOAA 10008 located just south-east of disk center at a distance of about 0.22 $R_{\odot}$. Sixteen scans were taken from 17:38 to 21:59 UT at a 15 minute cadence (with a longer gap near local noon for calibration and telescope repointing).

For the polarization measurements two Meadowlark liquid crystal variable retarders (LCVR) were used and modulated at about 4 Hz through a set of six retardance states to collect I+(Q,U,V) and I-(Q,U,V) spectral images. Prior to the observations, each LCVR was calibrated by measuring the transmitted intensity at 1565nm as a function of applied voltage when placed between crossed linear polariods. As the LCVRs were located behind the spectrograph slit in a low flux environment, no active temperature control was done. Since the telescope was continuously scanned during the polarization chopping, a temporally symmetric chopping sequence was used to minimize bias in the polarization measurements. A spectral flat field was produced from 40 quiet sun slit positions within each sunspot scan and processed

using an approach similar to Jones (2003). This spectral flat was used to correct the Stokes I frames, which produced a signal to noise ratio in Stokes I of nearly 100. The Stokes Q, U, and V frames were produced from simple differencing (which is very effective at removing systematic errors) and then a small correction for polarization dependent gain variations was made using a median of quiet Sun polarization frames. The noise levels in the Stokes Q, U, and V frames are comparable to each other, and roughly 0.6% of the continuum intensity.

The polarization frames shown in Figure 1 were taken with the spectrograph slit crossing the sunspot umbra at 17:36 UT. The left column of the figure shows the observed Stokes spectral frames, and the right column shows the corrected Stokes spectral frames as discussed in the following section. Visible are polarization signals in three atomic lines of Fe I, and also in molecular lines from OH.

3. Removing Instrumental Polarization

The Stokes vectors are defined as follows: positive Stokes Q is defined along the geocentric N-S direction, positive Stokes U is defined as $\frac{\pi}{4}$ counter-clockwise from positive Stokes Q, and positive Stokes V is defined such that Stokes V / dI/dλ is negative for the umbra of NOAO 10008 (consistent with MDI and NSO/KPVT magnetograms). Following Capitani et al. (1989) the observed Stokes vector $\vec{S'}$ is simply the product of the telescope Mueller matrix and the true (or input) Stokes vector $\vec{S'} = M\vec{S}$. The question of recovering the true Stokes vector is then a matter of determining the inverse Mueller matrix M^{-1}.

As discussed by Collados (2003) there are direct and indirect methods for determining the instrumental polarization. An indirect method was used first, based the decomposition discussed by Kuhn *et al.* (1994). With this method the observed σ component of the Stokes V line profile, which is strictly equal to zero in the physics of the Zeeman effect, is interpretted as arising from polarization cross-talk from the Stokes Q and U states. The decomposition proceded as follows: using spatial pixels in a scan from several places in the sunspot umbra where the Stokes V σ components were completely resolved and the Stokes Q and U π components showed differences, a regression technique was used to determine the cross-talk coefficients between the Stokes V and the Stokes Q and U states by fitting the observed line center Stokes V signal: $V'(\lambda_0) = aU'(\lambda_0) + bQ'(\lambda_0)$. The observed Stokes V was then corrected for the Stokes Q and U crosstalk using these two coefficients, producing a true solar Stokes V spectrum at all wavelengths, $V(\lambda) = V' - aU'(\lambda) - bQ'(\lambda)$. Next the crosstalk between

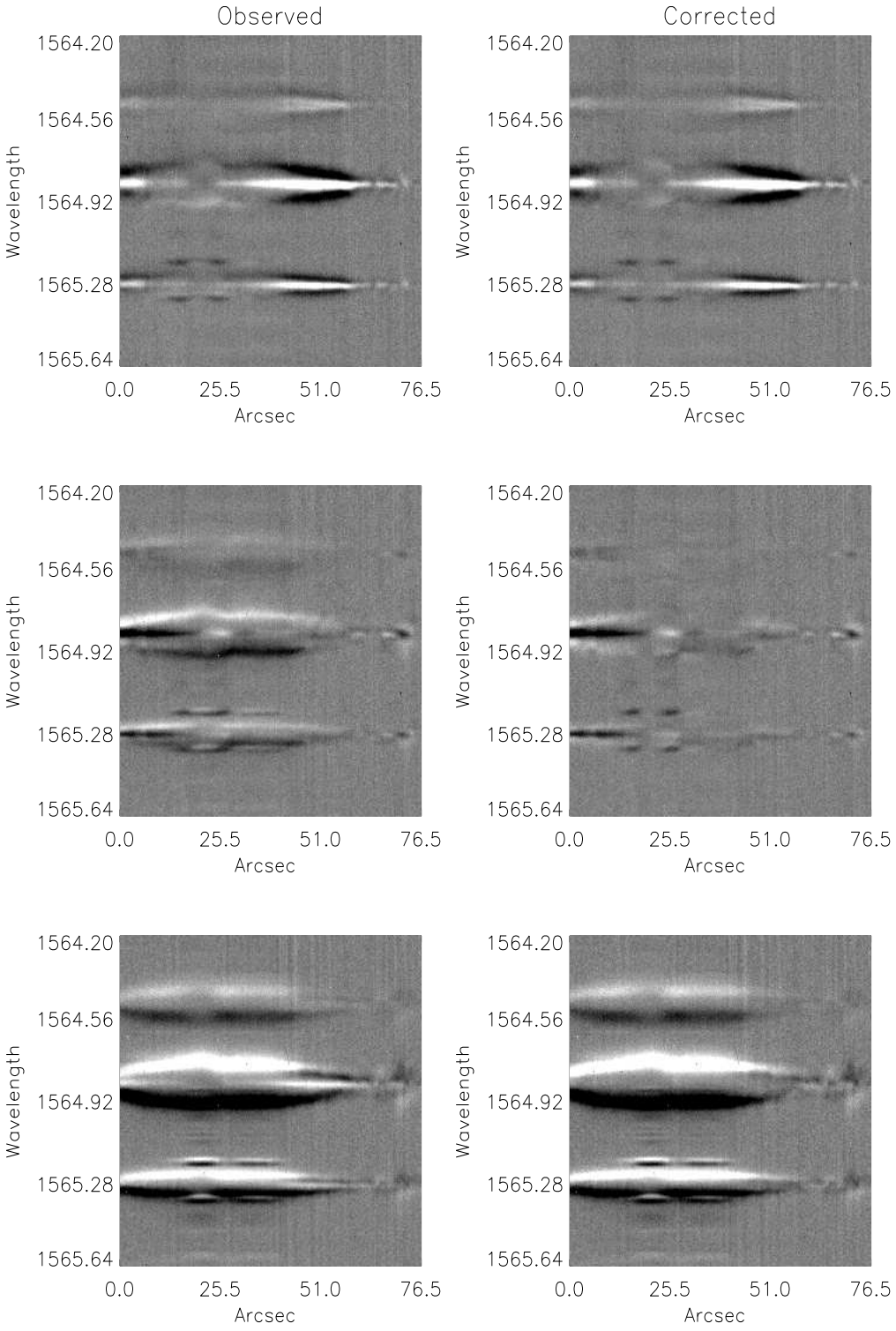

Figure 1. Observed and corrected Stokes U, Q, and V spectral frames from a slice through the umbra of NOAA 10008. Three Fe I absorption lines can be seen at 1564.5, 1564.8 and 1565.3nm, with the 1564.8nm line displaying the large Lande factor $g = 3$. Molecular absorption lines from OH are visible at 1565.1 and 1565.3nm.

the Stokes Q and V, and between the Stokes U and V was determined by fitting the U and Q spectra with the V spectrum and taking the median fit coefficient from several spatial pixels across the sunspot, $U(\lambda) = U'(\lambda) - cV(\lambda)$, and $Q(\lambda) = Q'(\lambda) - dV(\lambda)$, A very similar technique is used by Schlichenmaier and Collados (2002).

In each sunspot scan these four coefficients are determined from a single slit position and using only the Fe I 1564.8nm absorption line. These four coefficients were then used to correct the entire scan (200 slit positions) at all wavelengths. Sample observed and corrected spectral frames are shown in Figure 1. The coefficients can also be used to compute the inverse Mueller matrix, (actually the transpose of the inverse Mueller matrix as defined above) and by computing separate coefficients for each sunspot scan, a time sequence of the elements in the inverse Mueller matrix $M_K^{-1}(t)$ can be produced. The values for the time averaged inverse Mueller matrix for all of the observations was computed as:

$$\langle M_K^{-1} \rangle_t = \begin{pmatrix} 100.0 & 0.0 & 0.0 & 0.0 \\ 0.0 & 98.2 & 10.6 & -32.7 \\ 0.0 & 1.0 & 94.1 & 18.3 \\ 0.0 & 5.5 & -32.5 & 100.0 \end{pmatrix} \times 10^{-2}$$

Besides instrumental polarization crosstalk, polarization crosstalk originating in the solar atmosphere through magneto-optical effects (anomalous dispersion) can also make the observed polarization different from the true solar polarization. Instrumental polarization crosstalk is thought to dominate over magneto-optical effects in these observations for two main reasons. First, an examination of Figure 1 shows that all three Fe I lines in the spectral frame appear to be equally corrected. That is to say that all three corrected lines appear symmetric across line center in Stokes Q and U and anti-symmetric about line center in the Stokes V frame. This is true even though only the strongest line at 1564.8nm was used to compute the instrumental crosstalk. The amplitude of magneto-optical effects in a line varies as $\eta_0/\lambda g_{eff}$ (Skumanich and Lites, 1987a), where η_0 is the ratio of the line opacity to the continuum opacity. Each of these three Fe I spectral lines have different g_{eff} and since they each have different line center continuum depths it is likely they have different η_0, and so the amplitude of the magneto-optical effects in each line is expected to be different. If the instrumental correction derived from the Fe I 1564.8nm line were significantly contaminated by the magneto-optical effect, then that instrumental correction applied to the other Fe I lines would not be effective (for example it might over-correct the actual Stokes mixing in the other lines). Since all lines seem well corrected it is

assumed that the magneto-optical effect is much less than the observed instrumental crosstalk. Secondly, the amplitude of the magneto-optical matrix elements contains a dependence on the magnetic azimuth and inclination values (Skumanich and Lites, 1987b). Since the cross-talk coefficients here are determined with fit techniques using several spatial pixels across the sunspot (each with different azimuth and inclination angles) it is felt that this spatial sampling also makes this technique insensitive to magneto-optical contamination.

Mathematical models of the expected Mueller matrix for several telescopes have been made by various authors (Makita and Nishi 1970, Balasubramaniam, Venkatakrishnan and Bhattacharyya 1985, Capitani *et al.* 1989, Elmore *et al.* 1992, and Kuhn *et al.* 1994) and a model for the McMath-Pierce telescope itself is presented by Bernasconi (1997). A new simpler model is produced here based upon the mirror reflection Mueller matrix from Capitani et al. (1989), the telescope parameters discussed in Livingston and Harvey (1971), and the assumption that each mirror has an identical value for the complex index of refraction.

We apply this model using the computed solar position during 24 June 2002 to derive a telescope Mueller matrix for the times of each observation. Then this matrix is inverted to produce a time series of values for the model inverse Mueller matrix $M_m^{-1}(t)$. This model matrix was computed using a range of value for n and k, the complex indicies of refraction for the aluminum coating of the telescope mirrors, and a value for χ^2 is computed using the Stokes Q, U and V cross-talk values. The best fit values are found to be $n = 1.0$ and $k = 9.5$, and these values are used to model the telescope polarization. The time sequence of these model inverse Mueller matrix elements is then averaged to produce the mean model Mueller matrix as follows:

$$\langle M_m^{-1} \rangle_t = \begin{pmatrix} 103.4 & 3.2 & 0.0 & 0.0 \\ 3.2 & 103.3 & 0.0 & -0.2 \\ 0.0 & 0.1 & 98.7 & 30.5 \\ 0.0 & 0.2 & -30.5 & 98.7 \end{pmatrix} \times 10^{-2}$$

An inherent assumption in the Kuhn decomposition technique is that the cross-talk between the Stokes I and Stokes Q, U and V is zero. This means that the first row and column of the $M_K^{-1}(t)$ matrix would strictly equal $[1.0, 0, 0, 0]$. Comparison with the model matrix shows that this assumption is valid to the level of about 3%. It is likely that an attempt to directly measure these coefficients would be limited by the flat-field correction of the Stokes I spectra and a level near this value; further investigation of these terms is not done. With detectors where flat-fielding problems are significantly reduced, Bernasconi (1997) was able to compute and successfully model the Stokes I to Stokes Q, U

and V crosstalk directly. The decomposition method also assumes the Stokes V to V term is exactly 1.0, again this is accurate to about 3%. These terms are consistent with the results of Collados (2003), who studied several methods and found agreement between various techniques at the level of a few percent.

The middle diagonal elements of the matrices, and the lower left region of the matrices also agree to within about 3%. However, the values for $M_K^{-1}(2,3), (2,4)$ and $(3,4)$ show much larger differences from the model values. The time dependence of the $M_K^{-1}(2,3)$ and $M_K^{-1}(3,4)$ elements is similar to the model inverse Mueller matrix elements. It is likely that the 10% discrepancy between the actual and the predicted values is due to the simplicity of the model in these two cases. The behavior of the χ^2 fit for n and k discussed above shows that the value of n is not constrained very well. This suggests that using one value for these parameters for all the mirrors may be a poor assumption, and this is supported by the results of Bernasconi (1997). The time dependence of the $M_K^{-1}(2,4)$ matrix element is not similar to the model predictions however. It is thought that a problem with the polarimeter, which was not included in the model, is the culprit for the 30% discrepancy of this term. Clearly a better model is needed to fully understand the telescope polarization, but the correspondance of the Kuhn decompostion values with this simple model is encouraging. In all cases, the Kuhn decomposition values are used to calibrate the Stokes polarization spectra.

4. Magnetic Field Measurements

The instrument corrected 1564.8nm Fe I observations were inverted using the Skumanich and Lites (1987a) full Stokes least-squares fitting program. It uses a radiative source function which varies linearly with optical depth (Milne-Eddington atmosphere), assumes Voigt profiles for the spectral lines, and computes a mean magnetic vector for the entire line formation height in the solar atmosphere. This technique has been used by many authors in the past and is being implemented on NSO SOLIS Vector Spectromagnetograph observations of the 630.2nm Fe I line pair (Henney *et al.* 2003). Line parameters specific to the Fe I 1564.8nm line (with Landè factor g=3) and a relative weighting between the Stokes I (10%) and Stokes Q, U, and V (100%) spectra were used. Currently the software only fits the 1564.8nm line, but future work may additionally use the two neighboring Fe lines.

Two sample fits to the Stokes spectra are shown; the polarization spectra from a pixel in the sunspot umbra are shown in Figure 2, and

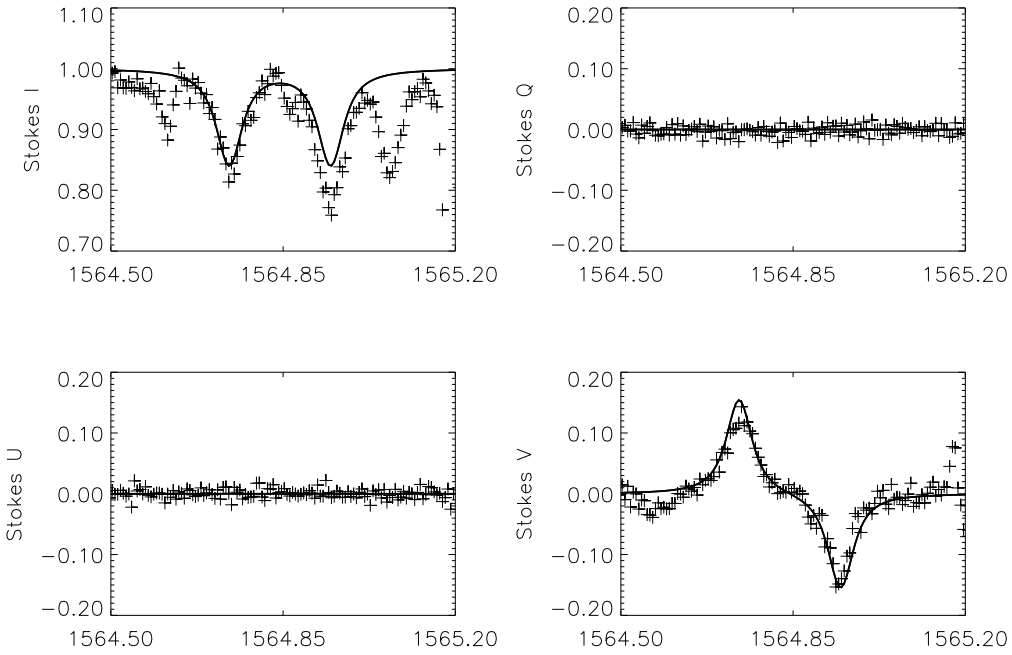

Figure 2. Stokes spectra from a typical pixel in the sunspot umbra (*crosses*) and the corresponding spectral fits from the inversion. Each plot is normalized by the continuum intensity in the umbra. Several nearby molecular spectral lines can be seen both to the blue and red wavelengths in the intensity plot which are not fit by the inversion.

those from a pixel in the sunspot penumbra are shown in Figure 3. The intensity spectrum contains several molecular absorption lines which are not included in the fit procedure. Due to this and the lower weighting given to the intensity spectrum, the fit is not as good as the fits to the polarization spectra. Since the sunspot was near disk center, the umbral spectra show magnetic fields directed mostly along the line-of-sight, with strong Stokes V and almost no Stokes Q or U signal. The penumbral pixel shows the opposite with only a weak Stokes V and strong linear components, since the field there is mostly directed transverse to the line-of-sight.

Maps of the derived magnetic field parameters of the total magnetic field, field inclination and azimuth, and a continuum image are shown in Figure 4. The sunspot displays two umbrae, with the northernmost umbra being darker, about 0.45 times the quiet sun intensity, with the brighter umbra about 0.55 times the quiet sun intensity. The darker umbra also has a larger magnetic field strength, a little less

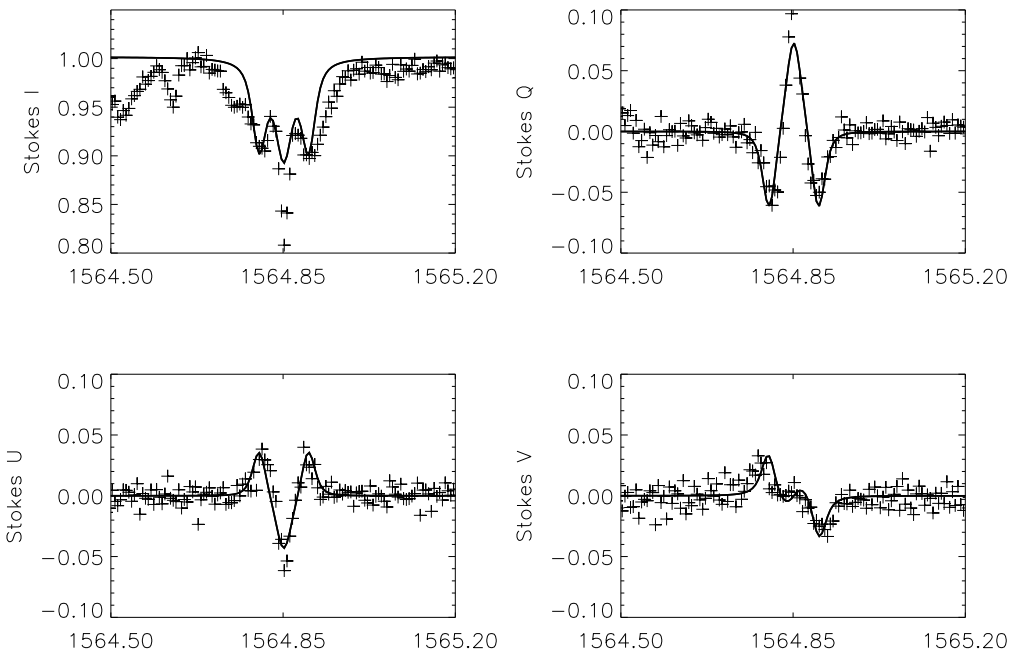

Figure 3. Stokes spectra from a typical pixel in the sunspot penumbra and the corresponding spectral fits from the inversion. As with the umbral spectrum, molecular absorption lines are seen in the intensity spectrum which are not fit in the inversion.

than 2800 Gauss, while the magnetic field is only measured at 2300 Gauss in southern umbra. The field strength drops to about 1200-1400 Gauss in the penumbra, and there are regions of 1200-1900G field strength outside of the main sunspot in other regions of the active region NOAA 10008.

The angle of inclination of the magnetic field measured from the line-of-sight ranges from roughly 0 degrees in the darkest umbra to about 10-15 degrees in the southern umbra, and then to nearly 90 degrees in the penumbra. The penumbral inclination shows a variation around the spot with the disk center side inclination being a few degrees less than the limb-ward penumbra, consistent with simple projection effects. Inside the penumbra are relatively narrow, radial regions of smaller inclination angle indicating magnetic fields which are more vertical than the surrounding horizontal penumbral fields. Previous observations of magnetic spines in the sunspot penumbra showed features which appear in both magnetic field strength and inclination angle (Lites *et al.* 1993), but in these observations of NOAA 10008 these spines are not obvious

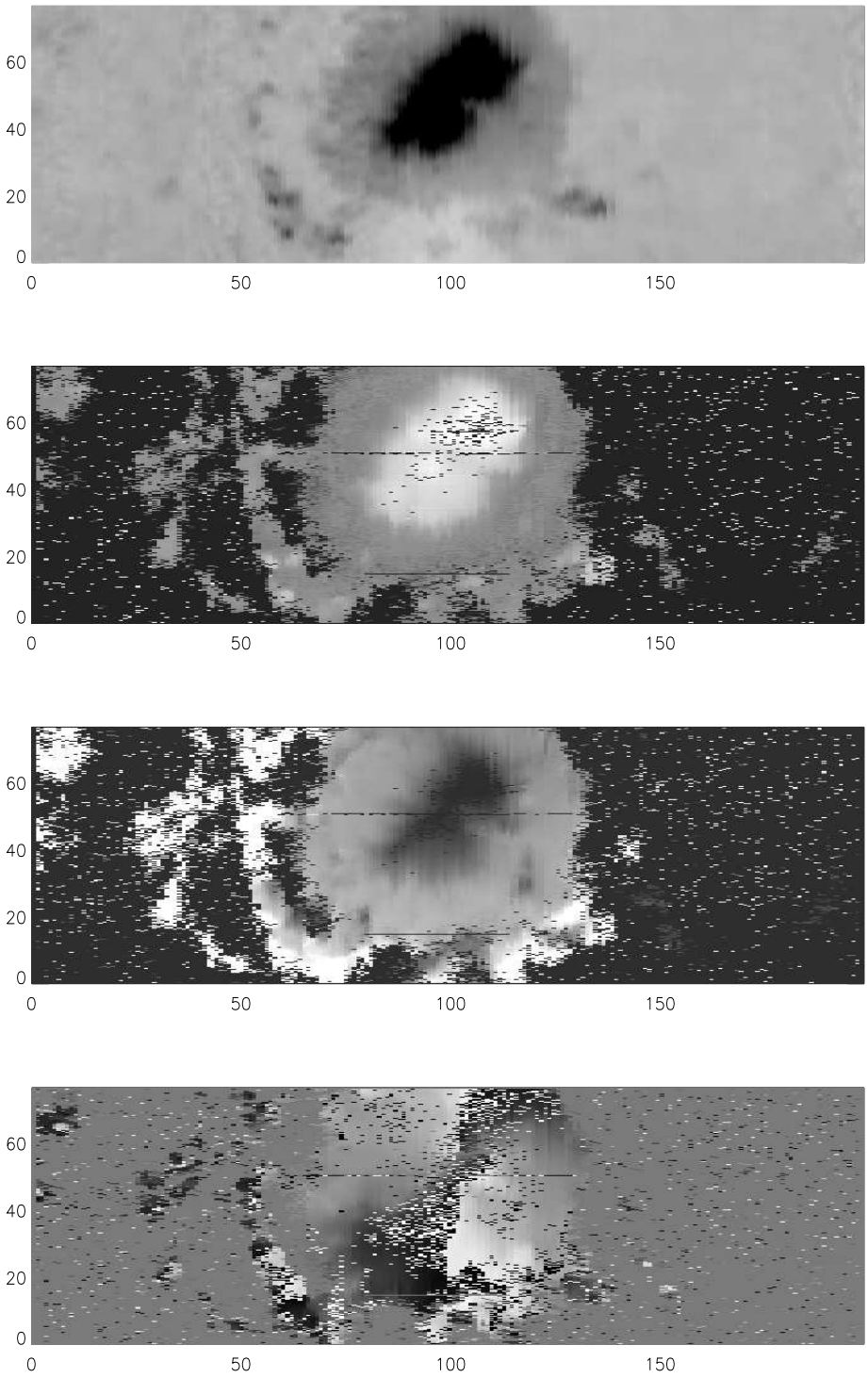

Figure 4. Maps of the sunspot region NOAA 10008 on 24 June 2002 and the associated magnetic field. From top to bottom are shown the continuum intensity at 1565nm, the magnetic field strength, the magnetic field inclination to the line-of-sight, and the azimuth angle of the transverse field. The sunspot is near disk center, geocentric north is up and east is left, and the axes are marked in arcseconds.

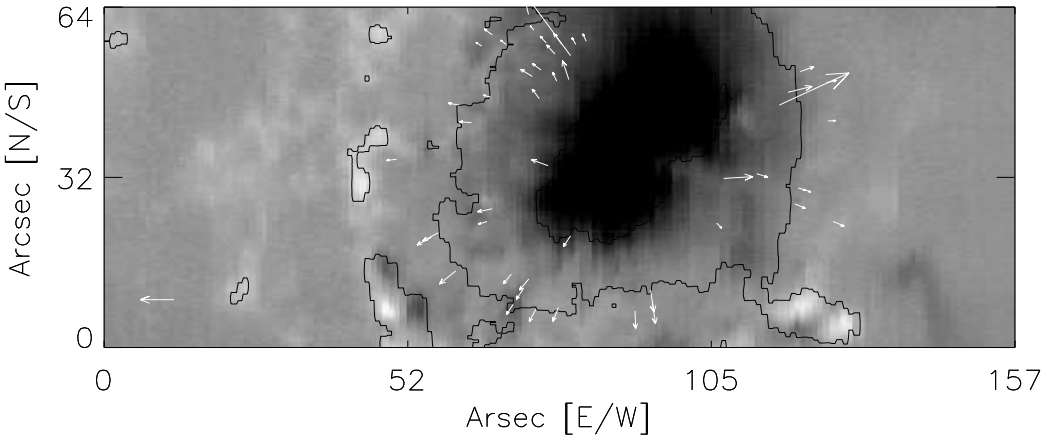

Figure 5. Vectors showing the velocity of MMF features and magnetic inclination features, superposed on a magnetogram image of the sunspot. The contours show the sunspot umbra and also the edge of the sunspot penumbra. The velocity vectors start at the initial position of the MMF feature, and the length of the vector is proportional to the radial speed. Surprisingly, about half of the MMF features are seen to start inside the sunspot penumbra. The vector at the lower left represents a speed of 1 km s^{-1}.

in the magnetic field strength maps. In addition to the magnetic spines, there are smaller spatial regions in the penumbra where the magnetic field inclination angle significantly varies from the typical horizontal direction. These regions have magnetic field inclinations of 40-60 degrees to the line of sight, and time sequences show that these features move outward through the penumbra with a radial velocity of about 0.4 km s^{-1}. They are often located between the magnetic spines in the regions of more horizontal magnetic field. The starting position of several of these moving penumbral inclination features and their relative radial velocities are shown in Figure 5. From visual inspection, ten of these features were clearly identified in the time sequence of magnetic field inclination angle. All ten features appeared clearly within the penumbral boundary of the sunspot, moved with a radial velocity of between 0.1 to 1.8 km s^{-1}, and tended to cluster at certain azimuth angles around the sunspot (which corresponded to the azimuth angles where most MMFs were observed).

A sequence of magnetograms were produced from the instrument corrected Stokes V spectra. The blue wing of the Fe I 1564.8nm line was integrated spectrally and subtracted from the integrated signal in the red wing of the line. The magnetogram from 17:36 UT is shown as

the background image in Figure 5. Magnetic spines in the penumbra are seen in these magnetograms, and pMMFs are visible at the same locations where the pMMFs are seen in the inclination angle maps. In the magnetogram time sequence, 38 MMFs are identified, about half of which appear inside the penumbra as pMMFs. The radial velocities for these features range from 0.2 to 2.5 km s^{-1}, and these features cluster at the same azimuth angles as the pMMFs seen in the magnetic inclination angle data. The median radial velocity is again 0.4 km s^{-1}, equal to the velocity observed for pMMFs (the median velocity, and the velocity ranges observed for these features are consistent with previous observations, such as Zhang, Solanki & Wang, 2003). In the penumbra it appears that these features are bipolar in the magnetogram maps (see Figure 6).

The pMMFs are most visible in the magnetogram time sequences, and they are not visible in the time sequences of total magnetic field strength, field azimuth, line center position or filling factor. As mentioned previously, the Stokes vectors are fit using a Milne-Eddington atmospheric model, and the routine produces maps of the two coefficients for the source function B_0 and μB_1 normalized by the continuum intensity, where $S = B_0 + B_1\tau$. In time sequences of the maps produced of these two coefficients, the pMMFs are very clearly seen in the μB_1 parameter. While the pMMFs are not visible in a time sequence of the continuum images, their visibility in the μB_1 parameter may indicate a temperature difference between the pMMFs and the surrounding penumbral plasma. Such a difference could indicate a direct relationship between these pMMFs and the moving penumbral intensity features seen in high resolution continuum images (Bovelet and Weihr, 2003).

Why haven't a large number of pMMFs been seen in previous studies of sunspots? Three possible explanations seem worth mentioning. First, it is possible that NOAA 10008 was observed at an unusual time or it was an unusual sunspot; however this is a rather unsatisfactory answer. Second, it is possible that the enhanced magnetic sensitivity of the Fe I 1564.8nm line (given by the ratio of the Zeeman splitting to the Doppler width) compared to the visible lines used in previous studies provides a more sensitive probe of these features. A third explanation is that the Fe I 1564.8nm line probes a deeper region of the solar atmosphere, and it is possible that at these lower layers pMMFs are more visible than at higher layers in the penumbral atmosphere. It is also possible that a combination of these factors is involved.

Moving penumbral magnetic features have not been directly addressed by models since they have not been mentioned in observations or represent only a tiny fraction of some observations. Almost all quan-

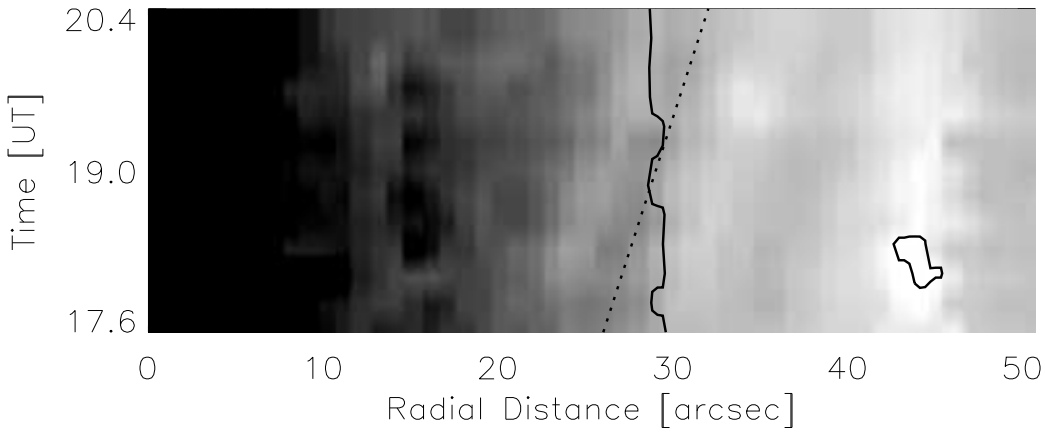

Figure 6. A time slice showing the radial motion of pMMFs and MMFs from the magnetogram movies of NOAA 10008. This figure was made by averaging a few azimuthal angles in the solar westward direction from the center of the sunspot umbrae. Alternating light an dark lines move from the outer half of the penumbra (dark bold line) outward into the surrounding quiet sun (the sunspot moat). The slope of line is 0.44 km^{-1} and is not a fit but merely illustrative of the typical velocity of these features.

titative or qualitative models of MMFs invoke a magnetic U-loop penetrating the solar photosphere with oppositely directed magnetic field lines which connect below the solar surface. These U-loops naturally produce the bi-polar magnetic quality of MMFs. A variety of U-loops have been examined with models, either upward rising (Spruit, Title & van Ballegooijen , 1987) or downward sinking (see Zhang, Solanki & Wang, 2003) U-loops. The sources of instabilities which form these loops from otherwise smooth magnetic field lines have been discussed by many authors and include sub-surface reconnection of active region field lines (Spruit, Title & van Ballegooijen 1987), flux pumping from granulation (Thomas *et al.* 2002), and a variety of instabilities caused by interaction of the Evershed mass flow and the horizontal magnetic field lines (Ryutova *et al.* 1997, Schlichenmaier, 2002 and Zhang, Solanki & Wang, 2003). While the fundamental physics involved in each model does not seem in conflict with the existence of pMMFs, none of these models directly address the issue of forming U-loops at a low altitude in the sunspot penumbra in regions of horizontal magnetic field lines. Future work is needed in this direction.

Acknowledgements

SAJ and SHL participated in this project through the the National Solar Observatory Research Experiences for Undergraduate (REU) site program, which is co-funded by the Department of Defense in partnership with the National Science Foundation REU Program. Thanks go to C. Plymate and E. Galayda for immeasureable help at the telescope during the observations. The CSUN-NSO camera was purchased using the AFOSR award F49620-00-1-0355. MJP thanks J. Harvey for a thorough reading of the manuscript, and W. Plick, B. Briggs, and W. Cao for help at McM/P during the summer 2002 observations.

References

Balasubramaniam, K., Venkatakrishnana, P., and Bhattacharyya, J.C.: 1985, *Solar Phys.* **99**, 333.

Bellot Rubio, L.R., Collados, M., Ruiz Cobo, B., and Rodrigues Hidalgo, I.: 2000, *Astrophys. J.* **534**, 989.

Bernasconi, P.N.: 1997, Diss ETH No. 12227.

Bovelet, B. and Wiehr, E.: 2003, *Astron. Astrophys.* **412**, 249.

Capitani, C., Cavallini, F., Ceppatelli, G., Landi Degl'Innocenti, E., Landi Degl'Innocenti, M., Landolfi, M. and Righini, A.: 1989, *Solar Phys.* **120**, 173.

Collados, M.: 2003, Polarimetry in Astronomy, ed S. Fineschi *SPIE* **4843** 55.

Elmore, D.F., Lites, B.W., Tomczyk, S., Skumanich, A.P., Dunn, R.B., Schuenke, J.A., Streander, K.V., Leach, T.W., Chambellan, C.W. and Hull, H.K.: 1992, *SPIE* **1746**, 22.

Harvey, J. and Harvey, K.: 1973, *Solar Phys.* **28**, 61.

Henney, C.J., Harvey, J.W., Keller, C.U., Jones, H.P., and the SOLIS Team : 2003, *BAAS* **35** #3, 808.

Jones, H.P.: 2003, *Solar Phys.* **218**, 1.

Kopp, G. and Rabin, D.: 1992, *Solar Phys.* **141**, 253.

Kuhn, J.R., Balasubramaniam, K., Kopp, G., Penn, M., Dombard, A. and Lin, H.: 1994, *Solar Phys.* **153**, 143.

Lin, H.: 1995, *Astrophys. J.* **446**, 421.

Lites, B.W., Elmore, D.F., Seagraves, P., and Skumanich, A.P.: 1993, *Astrophys. J.* **418**, 928.

Lites, B.W., Thomas, J.H., Bogdan, T.J. and Cally, P.S.: 1998 *Astrophys. J.* **497**, 464.

Livingston, W. and Harvey, J.: 1971, Kitt Peak National Observatory Contributions No. 558.

Makita, M. and Nishi, K.: 1970, *Ann. Tokyo Astron. Obs.* **12**, 121.

Mathew, S.K., Lagg, A., Solanki, S.K., Collados, M., Borrero, J.M., Berdyugina, S., Krupp, N., Woch, J., and Frutiger, C.: 2003, *Astron. Astrophys.* **410**, 695.

Mickey, D., Canfield, R.C., LaBonte, B.J., Leka, K.D, Waterson, M.F. and Weber, H.M.: 1996, *Solar Phys.* **168**, 229.

Pierce, A.K.: 1964, *Applied Optics* **3**, 1337.

Penn, M.J., Walton, S.R., Chapman, G., Ceja, J., and Plick, W.: 2003, *Solar Phys.* **213**, 55.
Ruiz Cobo, B. and del Toro Iniesta, J.C.: 1992, *Astrophys. J.* **398**, 375.
Ryutova, M., Shine, R., Title, A. and Sakai, J.I.: 1997, *Astrophys. J.* **492**, 402.
Sanakarasubramanian, K., Gullixson, C., Hegwer, S., Fletcher, S., Richards, K., Rousset, E., Lites, B.W., Elmore, D.F., Streander, K.V., and Sigworth, M.: 2004, *SPIE* **5171**, 207.
Schlichenmaier, R.: 2002, *Astron. Nachr.* **323**, 303.
Schlichenmaier, R. and Collados, M.: 2002, *Astron. Astrophys.* **381**, 668.
Skumanich, A., and Lites, B.: 1987a, *Astrophys. J.* **322**, 473.
Skumanich, A., and Lites, B.: 1987b, *Astrophys. J.* **322**, 483.
Spruit, H.C., Title, A.M. and van Ballegooigen, A.A.: 1987, *Sol. Phys.* **110**, 115.
Thomas, J. H., Weiss, N. O., Tobias, S. M., and Brummell, N. H.: 2002, *Nature* **420**, 390.
Title, A.M., Frank, Z.A., Shine, R.A., Tarbell, T.D., Topka, K.P., Scharmer, G., and Schmidt, W.: 1993, *Astrophys. J.* **403**, 780.
Walton, S.R., and Chapman, G.A.: 1996, *Solar Phys.* **166**, 267.
Zhang, J., Solanki, S.K., and Wang, J.: 2003, *Astron. Astrophys.* **399**, 755.